Viscosities of quark-gluon plasmas

H. Heiselberg
Nuclear Science Division, MS 70A-3307, Lawrence Berkeley Laboratory, Berkeley, California 94720
(Received 3 December 1993)

The quark and gluon viscosities are calculated in quark-gluon plasmas to leading orders in the coupling constant by including screening. For weakly interacting QCD and QED plasmas, dynamical screening of transverse interactions and Debye screening of longitudinal interactions controls the infrared divergences. For strongly interacting plasmas other screening mechanisms taken from lattice calculations are employed. By solving the Boltzmann equation for quarks and gluons including screening, the viscosity is calculated to leading orders in the coupling constant. The leading logarithmic order is calculated exactly by a full variational treatment. The next to leading orders are found to be important for the transport properties of quark-gluon plasmas created in relativistic heavy-ion collisions and the early universe, where the coupling constant is large.

PACS number(s): 12.38.Mh, 12.38.Bx, 21.65.+f, 95.30.Cq

I. INTRODUCTION

Transport and relaxation properties of quark and gluon (QCD) plasmas are important in a number of a different contexts. They determine the time that it takes a quark-gluon plasma formed in a heavy-ion collision to approach equilibrium, and they are of interest in astrophysical situations such as the early Universe, and possibly neutron stars.

The basic difficulty in calculating transport properties of such plasmas, as well as of relativistic electron-photon (QED) plasmas, is the singular nature of the long-range interactions between constituents, which leads to divergences in scattering cross sections similar to those found in Rutherford scattering. This makes the problem of fundamental methodological interest, in addition to its possible applications. The first approaches to describe the transport properties of quark-gluon plasmas employed the relaxation-time approximation [1–3] for the collision term. This approximation simplifies the collision integral enormously and transport coefficients are related directly to the relaxation time. The latter is typically estimated from a characteristic cross section times the density of scatterers. In Refs. [2, 3] the divergent part of the total cross section at small momentum transfers was assumed to be screened at momentum transfers less than the Debye momentum. However, Debye screening influences only the longitudinal (electric) part of the QED and QCD interactions, and the transverse (magnetic) part is unscreened in the static limit at order gT. It may be screened at order g^2T.

Recently it has been shown that the physics responsible for cutting off transverse interactions at small momenta is dynamical screening [4]. This effect is due to Landau damping of the exchanged gluons or photons. Within perturbative QCD and QED rigorous analytical calculations of transport coefficients to leading order have been made for high temperatures [4, 5] as well as low temperatures [6] as compared to the chemical potentials of the constituents.

Transport processes depend on a characteristic relaxation time, τ_{tr}, of the particular transport process considered. For example, in high-temperature plasma the viscosities, $\eta_i = w_i\tau_{\eta,i}/5$, of particle type i are proportional to the characteristic times for viscous relaxation, $\tau_{\eta,i} \sim \tau_{tr}$, which were first calculated in [4] to leading order in the coupling constant. More generally one finds that the typical transport relaxation rates that determine momentum stopping and thermal and viscous relaxation are in a weakly interacting QCD plasma:

$$\frac{1}{\tau_{tr}} \propto \alpha_s^2 \ln(1/\alpha_s)T + O(\alpha_s^2)\,, \tag{1}$$

where the expansion is in terms of the fine-structure constant $\alpha_s = g^2/4\pi$. The coefficients of proportionality to the leading order in α_s (in the following called the leading logarithmic order) has been calculated analytically for a number of transport processes in high-temperature plasmas [4, 5]. Likewise in a QED plasma the typical transport relaxation rates for viscous processes, momentum stopping, and thermal and electrical conduction have the same dependence as (1) on the QED fine-structure constant α [5].

The dependence of the transport rates on the coupling constants is very sensitive to the screening. In addition to the factor α_s^2 from the matrix element squared of the quark and gluon interactions, the very singular QCD interactions for small momentum transfers lead to a logarithm, $\ln(q_{\max}/q_{\min})$, of the maximum and minimum momentum transfers. The typical particle momenta limits the maximum momentum transfer, $q_{\max} \sim T$, and Debye and dynamical screening leads to effective screening for small momentum transfers of order $q_{\min} \sim q_D \sim gT$. This gives the leading logarithmic order in the coupling constant, $\ln(T/q_D) \sim \ln(1/\alpha_s)$, to the transport rates (1).

The calculations in [4, 5] were brief and dealt only with the leading logarithmic order in the coupling constant with a given ansatz for the distribution function. Here, more detailed calculations of the quark and gluon viscosities in the high-temperature quark-gluon plasmas are presented. The leading logarithmic order is calculated ex-

actly by a variational method and the next to leading order, the α_s^2 term in (1), is calculated as well. Because α_s is not exponentially small, the next to leading order is important in many realistic physical situations such as relativistic heavy-ion collisions and the early Universe. Furthermore when the Debye screening length is larger than the interparticle screening, which occurs when $\alpha_s \gtrsim 0.1$ as we shall see below, Debye and dynamical screening breaks down. Instead lattice gauge calculations have found that quark-gluon plasmas seem to develop a constant screening mass, $m_{\rm pl} \simeq 1.1T$, for temperatures $T \gtrsim 2-3T_c$, and it is important to see what effects this alternative screening mechanism has in strongly interacting plasmas.

We shall first describe in Sec. II the transport theory we use, namely, the Boltzmann equation, and the screening of long range QCD and QED interactions. In Sec. III, we describe the process of shear flow and the variational calculation necessary in order to find the viscosity. In Sec. IV we then evaluate the collision term to leading logarithmic order with a simplifying ansatz for the trial function and refer to Appendix A for a full and exact variational calculation. In Sec. V we calculate the viscosity to higher orders in the coupling constant and discuss strongly interacting plasmas. Finally, in Sec. VI we give a summary and discuss generalizations of the methods developed here to other transport coefficients.

II. TRANSPORT THEORY

Transport processes are most easily described by the Boltzmann equation

$$\left(\frac{\partial}{\partial t} + \mathbf{v}_1 \cdot \nabla_{\mathbf{r}} + \mathbf{F} \cdot \nabla_{\mathbf{p}_1}\right) n_1 = 2\pi\nu_2 \sum_{234} |M|^2 \times [n_1 n_2 (1 \pm n_3)(1 \pm n_4) - (1 \pm n_1)(1 \pm n_2) n_3 n_4] \times \delta(\epsilon_1 + \epsilon_2 - \epsilon_3 - \epsilon_4) \delta_{\mathbf{p}_1+\mathbf{p}_2;\mathbf{p}_3+\mathbf{p}_4} , \quad (2)$$

where ϵ_i is the energy and $\mathbf{p}_i$ the momentum of the quasiparticles, $\mathbf{F}$ some force acting on the quasiparticles, and the right-hand side of (2) is the collision term. $n_i(\mathbf{p}_i)$ are the Fermi and Bose quasiparticle distribution functions for quarks and gluons, and the signs $\pm$ include stimulated emission and Pauli blocking. The spin and color statistical factor ν_2 is 16 for gluons and $12N_f$ for quarks and antiquarks with N_f flavors. $|M|^2$ is the squared matrix element for the scattering process $12 \to 34$, summed over final states and averaged over initial states. It is related to the Lorentz-invariant matrix element $|\mathcal{M}|^2$ by $|M|^2 = |\mathcal{M}|^2/(16\epsilon_1\epsilon_2\epsilon_3\epsilon_4)$. For gluon-gluon scattering [7] (see Fig. 1),

$$|\mathcal{M}_{gg}|^2 = \frac{9}{4} g^4 \left(3 - \frac{us}{t^2} - \frac{st}{u^2} - \frac{ut}{s^2}\right) , \quad (3)$$

where s, t, and u are the usual Mandelstam variables. In Eq. (3) the double counting of final states has been corrected for by inserting a factor 1/2. For quark-gluon scattering,

$$|\mathcal{M}_{gq}|^2 = g^4 (u^2 + s^2) \left(\frac{1}{t^2} - \frac{4}{9us}\right) , \quad (4)$$

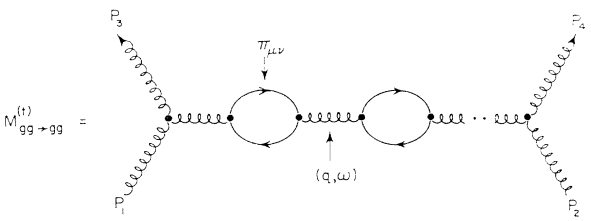

FIG. 1. Feynman diagram for gluon-gluon scattering in the t channel. The lines in the loops can be either quark or gluon propagators.

and for scattering of two different quark flavors,

$$|\mathcal{M}_{q_1 q_2}|^2 = \frac{4}{9} g^4 \frac{u^2 + s^2}{t^2} . \quad (5)$$

The matrix element for scattering of the same quark flavors or quark-antiquark scattering is different at large momentum transfer, but the same as (5) at small momentum transfers.

The t^{-2} and u^{-2} singularities in Eqs. (3)–(5) lead to diverging transport cross sections and therefore vanishing transport coefficients. Including screening, it was shown in [4–6] that finite transport coefficients are obtained. In fact, the leading contribution to transport coefficients comes from these singularities. In the $t = \omega^2 - q^2$ channel the singularity occurs for small momentum $\mathbf{q}$ and energy ω transfers (see Fig. 1).

For small momentum transfer, $q \ll \epsilon_1, \epsilon_2 \sim T$, energy conservation implies that $\omega = \epsilon_1 - \epsilon_3 \simeq \mathbf{v}_1 \cdot \mathbf{q} = -\mathbf{v}_2 \cdot \mathbf{q}$, where $\mathbf{v}_i = \mathbf{p}_i$. Therefore the velocity projections transverse to $\mathbf{q}$ have lengths $|\mathbf{v}_{1,T}| = |\mathbf{v}_{2,T}| = \sqrt{1-\mu^2}$, where $\mu = \omega/q$. Consequently, $\mathbf{v}_{1,T} \cdot \mathbf{v}_{2,T} = (1-\mu^2)\cos\phi$, where ϕ is the angle between $\mathbf{v}_{1,T}$ and $\mathbf{v}_{2,T}$. For $q \ll T$ we thus have

$$s \simeq -u \simeq 2p_1 p_2 (1 - \cos\theta_{12}) \simeq 2p_1 p_2 (1-\mu)(1-\cos\phi) , \quad (6)$$

and the interactions split into longitudinal and transverse ones [8]:

$$|M_{gg}|^2 = \frac{9}{8} g^4 \left| \frac{1}{q^2 + \Pi_L} - \frac{(1-\mu^2)\cos\phi}{q^2 - \omega^2 + \Pi_T} \right|^2 . \quad (7)$$

The interactions are modified by inclusion of the gluon, or photon, self-energies Π_L and Π_T [8] (see also Fig. 1). In the random-phase approximation (RPA) the polarizations are given in the long-wavelength limit ($q \ll T$) by

$$\Pi_L(q,\omega) = q_D^2 \left[1 - \frac{\mu}{2} \ln\left(\frac{\mu+1}{\mu-1}\right)\right] , \quad (8)$$

$$\Pi_T(q,\omega) = q_D^2 \left[\frac{\mu^2}{2} + \frac{\mu(1-\mu^2)}{4} \ln\left(\frac{\mu+1}{\mu-1}\right)\right] , \quad (9)$$

where $\mu = \omega/q$ and $q_D = 1/\lambda_D$ is the Debye wave number. In a weakly interacting high-temperature QCD plasma [8, 9],

$$q_D^2 = 4\pi(1 + N_f/6)\alpha_s T^2 , \tag{10}$$

where $\alpha_s = g^2/4\pi$ is the fine-structure constant for strong interactions, the factor $(1 + N_f/6)$ is the sum of contributions from gluon screening, the "1," and from light-mass quarks, of number of flavors, N_f. In a high-temperature QED plasma, $q_D^2 = 4\pi\alpha T^2/3$, where α is the QED fine-structure constant.

One should keep in mind that the self energies of (8) and (9) are only valid in the long-wavelength limit, i.e., for $q \ll T$. When $q \sim T$ other contributions of order $\alpha_s qT$ enter (see, e.g., [8]) which may be gauge dependent [10]. However, as long as α_s is small all contributions from the self-energies can be ignored in the gluon propagator when $q \sim T$ because the matrix element squared already carries the order α_s^2.

In the above derivations we have consistently assumed that the screening was provided in the RPA by the gluon self-energies, which give the Debye and dynamical screening of longitudinal and transverse interactions, respectively. Both effects provide a natural effective cutoff of momentum transfer less than $q_{\min} \sim q_D$. These perturbative ideas must, however, break down when the screening length becomes as short as the interparticle spacing, i.e., when $q_D \sim T$. In terms of the coupling constant this breakdown happens when $\alpha_s \gtrsim [4\pi(1 + N_f/6)]^{-1} \sim 0.1$, according to Eq. (10). In lattice gauge calculations of quark-gluon plasma above twice the temperature of the phase transition, $T_c \simeq 180$ MeV, one finds strong nonperturbative effects in the plasma so that the typical screening mass is $m_{\rm pl} \sim 1.1T$ [11]. One may argue [12] that perturbation theory still applies for large momentum transfers so that the matrix elements are given by the simple Feynman tree diagrams, but that perturbation theory does not apply for small momentum transfers of order $q \lesssim q_D$, and that one should rather insert the effective cutoff found by lattice gauge calculations

$$\Pi_L \simeq \Pi_T \simeq m_{\rm pl} , \quad \alpha_s \gtrsim 0.1 . \tag{11}$$

As will be shown below, the transport rates depend only logarithmically on the cutoff. The phenomenological screening mass of (11) provides us with a method to extend our calculations of transport coefficients to larger values for α_s, and it can be combined to the Debye and dynamical screening in weakly interacting quark-gluon plasmas.

III. THE VISCOSITY

With screening included in the interaction we can now proceed to calculate transport properties as the viscosity. In the presence of a small shear flow, $\mathbf{u}(y)$, in the x direction we obtain from the Boltzmann equation

$$p_{1x}v_{1y}\frac{\partial n_1}{\partial \epsilon_1}\frac{\partial u_x}{\partial y} = 2\pi\nu_2 \sum_{234} |M|^2[n_1 n_2(1 \pm n_3)(1 \pm n_4) - (1 \pm n_1)(1 \pm n_2)n_3 n_4] \times \delta(\epsilon_1 + \epsilon_2 - \epsilon_3 - \epsilon_4)\delta_{\mathbf{p}_1+\mathbf{p}_2;\mathbf{p}_3+\mathbf{p}_4} . \tag{12}$$

For small $\mathbf{u}$ we can furthermore linearize the quasiparticle distribution function

$$n_i = n_i^{\rm LE} + \frac{\partial n}{\partial \epsilon_p}\Phi_i \frac{\partial u_x}{\partial y} , \tag{13}$$

where the local equilibrium distribution function is

$$n_i^{\rm LE} = \{\exp[(\epsilon_i - \mathbf{u}\cdot\mathbf{p}_i)/T] \mp 1\}^{-1} , \tag{14}$$

and Φ_i is an unknown function that represents the deviations from local equilibrium. By symmetry Φ has to be on the form

$$\Phi = \hat{p}_x\hat{p}_y f(p/T) , \tag{15}$$

where now the function f must be determined from the Boltzmann equation. Inserting (13) in the Boltzmann equation we find

$$p_{1x}v_{1y}\frac{\partial n_1}{\partial \epsilon_1} = 2\pi\nu_2 \sum_{234} |M|^2[n_1 n_2(1 \pm n_3)(1 \pm n_4) - (1 \pm n_1)(1 \pm n_2)n_3 n_4] \times \delta(\epsilon_1 + \epsilon_2 - \epsilon_3 - \epsilon_4)\delta_{\mathbf{p}_1+\mathbf{p}_2;\mathbf{p}_3+\mathbf{p}_4} \times (\Phi_1 + \Phi_2 - \Phi_3 - \Phi_4) . \tag{16}$$

It is very convenient to define a scalar product of two real functions by

$$\langle\psi_1|\psi_2\rangle = -\nu_2 \sum_{\mathbf{p}} \psi_1(\mathbf{p})\psi_2(\mathbf{p})\frac{\partial n}{\partial \epsilon_p} . \tag{17}$$

Thus Eq. (16) may be written on the form $|X\rangle = I|\Phi\rangle$, where $|X\rangle = p_x v_y$ and I is the integral operator acting on Φ. The viscosity is given in terms of Φ [13] and can now be written as

$$\eta = -\nu_2 \sum_{\mathbf{p}} p_x v_y \frac{\partial n}{\partial \epsilon_p}\Phi_{\mathbf{p}} = \langle X|\Phi\rangle . \tag{18}$$

Equivalently, the viscosity is given from (16) as

$$\eta = \frac{\langle X|\Phi\rangle^2}{\langle\Phi|I|\Phi\rangle} . \tag{19}$$

Since $\langle .|.\rangle$ defines an inner product, the quantity $\langle X|\Psi\rangle^2/\langle\Psi|I|\Psi\rangle$ is minimal for $\Psi = \Phi$ with the minimal value η. Equation (19) is therefore convenient for variational treatment, which will be carried out in Appendix A.

To find the viscosity we must solve the integral equa-

tion (16) for which we have to evaluate

$$\langle\Phi|\ I\ |\Phi\rangle = 2\pi\nu_2 \sum_{\mathbf{p}_1,\mathbf{p}_2,\mathbf{q}} |M|^2 n_1 n_2 (1\pm n_3)(1\pm n_4) \times \frac{(\Phi_1+\Phi_2-\Phi_3-\Phi_4)^2}{4}\delta(\epsilon_1+\epsilon_2-\epsilon_3-\epsilon_4)\,. \quad (20)$$

Momentum conservation requires that $\mathbf{p}_3 = \mathbf{p}_1 + \mathbf{q}$ and $\mathbf{p}_4 = \mathbf{p}_2 - \mathbf{q}$ where $\mathbf{q}$ is the momentum transfer. Introducing an auxiliary integral over energy transfers, ω, the δ function in energy can be written

$$\delta(\epsilon_1+\epsilon_2-\epsilon_3-\epsilon_4) = \int d\omega \frac{p_3}{p_1 q}\delta\left(\cos\theta_1 - \mu - \frac{t}{2p_1 q}\right) \times \frac{p_4}{p_2 q}\delta\left(\cos\theta_2 - \mu + \frac{t}{2p_2 q}\right), \quad (21)$$

where θ_1 is the polar angle between $\mathbf{q}$ and $\mathbf{p}_1$ and θ_2 is the corresponding one between $\mathbf{q}$ and $\mathbf{p}_2$ (see Fig. 2). Consequently, we find

$$\langle\Phi|I|\Phi\rangle = \frac{1}{4\pi^8 T}\int_0^\infty dq \int_{-q}^{q} d\omega \times \int_{(q-\omega)/2}^{\infty} dp_1\, p_1^2 n_1(p_1)[1\pm n_1(p_1+\omega)] \times \int_{(q+\omega)/2}^{\infty} dp_2\, p_2^2 n_2(p_2)[1\pm n_2(p_2-\omega)] \times \int_0^{2\pi}\frac{d\phi}{2\pi}|M|^2(\Phi_1+\Phi_2-\Phi_3-\Phi_4)^2\,. \quad (22)$$

This integral equation for Φ has been solved in a few cases under simplifying circumstances. For example, in Fermi liquids the sharp Fermi surface restricts all particle momenta near the Fermi surface, and with a simplified form for the scattering matrix element techniques have been developed to calculate a number of transport coefficients exactly [13]. For the QCD and QED plasmas the very singular interaction can, once screened, be exploited since it allows an expansion at small momentum transfers. Thus an analytical calculation of the transport coefficients can be carried out at least to leading logarithmic order in the coupling constant [4–6].

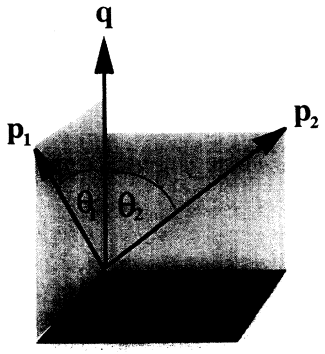

FIG. 2. The collision geometry. For small momentum transfer, $q \ll p_1, p_2$, energy and momentum conservation requires $\cos\theta_1 = \cos\theta_2 = \omega/q$.

IV. VISCOSITY TO LEADING LOGARITHMIC ORDER

In Ref. [4], through solution of the Boltzmann kinetic equation, the first viscosity of a quark-gluon plasma was derived to leading logarithmic order in the QCD coupling strength. We will in the following give a more thorough and exact derivation of the quark and gluon viscosity. The total viscosity, to leading order, is an additive sum of the gluon and quark viscosities, $\eta = \eta_g + \eta_q$.

The leading logarithmic order comes from small momentum transfers because the very singular matrix element (7) dominates. For small q the kinematics simplify enormously and, as we will now show, the integrals separate allowing almost analytical calculations. First, we can set the lower limits on the p_1 and p_2 integrals to zero, however, then replacing the upper limit on q by the natural cutoff from the distribution functions, which is $q_{\max} \sim T$. Thus we find, from (22),

$$\langle\Phi|I|\Phi\rangle = \frac{1}{2\pi^8 T}\int_0^\infty dp_1\, p_1^2 n_1(1\pm n_1) \times \int_0^\infty dp_2\, p_2^2 n_2(1\pm n_2) \times \int_0^{q_{\max}} q dq \int_{-1}^{1}\frac{d\mu}{2}\int_0^{2\pi}\frac{d\phi}{2\pi} \times |M|^2(\Phi_1+\Phi_2-\Phi_3-\Phi_4)^2\,, \quad (23)$$

to leading logarithmic order

The solution to the integral equation or equivalently the variational calculation of (19) is quite technical and is for that reason given in Appendix A. A much simpler calculation is to make the standard assumption in viscous processes, i.e., to take the trial function as

$$f(p/T) = (p/T)^2\,. \quad (24)$$

As will be shown in Appendix A this turns out to be a very good approximation. It is accurate to more than 99% for reasons also explained in the appendix. f can be defined up to any constant which cancels in (19) and therefore never enters in the viscosity.

The quantity $(\Phi_1+\Phi_2-\Phi_3-\Phi_4)^2$ can be averaged over x and y directions while keeping μ and ϕ fixed. This corresponds to keeping the relative positions of the three vectors $\mathbf{q}$, $\mathbf{p}$, and $\mathbf{p}'$ fixed relative to each other and rotating this system over the three Euler angles (see also Appendix A). Consequently, we obtain

$$\langle(\Phi_1+\Phi_2-\Phi_3-\Phi_4)^2\rangle = \frac{q^2}{15T^4}\{3(\mathbf{p}_2-\mathbf{p}_1)^2 + [\hat{\mathbf{q}}\cdot(\mathbf{p}_2-\mathbf{p}_1)]^2\} = \frac{q^2}{15T^4}\{(3+\mu^2)(p_1^2+p_2^2) - 2p_1p_2[4\mu^2+3(1-\mu^2)\cos\phi]\}. \quad (25)$$

The integrals over p_1 and p_2 in (23) are elementary. Next we perform the integrations or averages over μ and ϕ required in (23). We note in passing that the term in (25) proportional to p_1p_2 vanishes and that μ^2 effectively can

be replaced by 1/3 (see Appendix A). Let us first consider the case of gluon-gluon scattering inserting $|M_{gg}|^2$ from (3). We thus find

$$\langle\Phi|I|\Phi\rangle = \frac{2^8\pi^3}{45}\alpha_s^2 T^3 \int_0^{q_{\max}} q^3 dq \int_0^1 d\mu \times \left[\frac{1}{|q^2+\Pi_L(\mu)|^2} + \frac{1/2}{|q^2+\Pi_T(\mu)/(1-\mu^2)|^2}\right]. \tag{26}$$

This integral is discussed in detail in Appendix B. For the longitudinal interactions $\Pi_L \simeq q_D^2$ due to Debye screening and the leading term is a logarithm of the ratio of maximum to minimum momentum transfer, $\ln(q_{\max}/q_{\min}) \sim \ln(T/q_D)$. Likewise for the transverse interactions $\Pi_T \simeq i(\pi/4)\mu q_D^2$ due to Landau damping and the dependence on $\mu = \omega/q$ provides sufficient screening to render the integral finite, and the leading term is the same logarithm as for the longitudinal interactions. Whereas the details of the screening are unimportant for the leading logarithmic order, they are important for the higher orders and they are calculated in detail in Appendix B. The final result is thus, to leading logarithmic order,

$$\langle\Phi|I|\Phi\rangle = \frac{2^7\pi^3}{15}\alpha_s^2 \ln(T/q_D) T^3\,, \tag{27}$$

Since $\langle\Phi|X\rangle = [64\xi(5)/\pi^2]T^3$, we find, from (19) and (27),

$$\eta_{gg} = \frac{2^5 15\xi(5)^2}{\pi^7}\frac{T^3}{\alpha_s^2\ln(T/q_D)} \simeq 0.342\frac{T^3}{\alpha_s^2\ln(1/\alpha_s)}\,, \tag{28}$$

to leading logarithmic order in $\alpha_s = g^2/4\pi$.

To obtain the full gluon viscosity we must add scattering on quarks and antiquarks, which is calculated analogously and only has a few factors different. Firstly, from (3) and (4) we see that the matrix element squared is a factor 4/9 smaller. Secondly, the statistical factor is $\nu_2 = 12N_f$ instead of 16. Thirdly, in integrating over the factor $(p_1^2+p_2^2)$ in Eq. (25) we note that the distribution function, n_2, in Eq. (23) is now a fermion one. Consequently, the p_1 and p_2 integrations give a factor $(1/2+7/8)/2$ less for gluon-quark collisions as compared to gluon-gluon collisions and we find

$$\eta_g = (\eta_{gg}^{-1}+\eta_{gq}^{-1})^{-1} = \frac{\eta_{gg}}{1+11N_f/48}. \tag{29}$$

In [4] the slightly different result $\eta_g = \eta_{gg}/(1+N_f/6)$ was obtained.

The quark viscosity can be obtained analogously to the gluon one. The quark viscosity due to collisions on quarks only, η_{qq}, deviates from η_{gg} by a factor $(4/9)^2$ in the matrix elements. In addition another factor appears because Fermi integrals are involved instead of Bose integrals. By comparing to (19,18,20) we find

$$\eta_{qq} = \eta_{gg}\frac{(15/16)^2}{(4/9)^2(7/8)(1/2)} = \eta_{gg}\frac{5^2 3^6}{2^8 7}\,. \tag{30}$$

Note that the statistical factors ν cancel in η_{gg} and η_{qq}. Including quark scatterings on gluons lead to similar factors in in $\langle\Phi|I|\Phi\rangle$, namely a factor (9/4) from the matrix element, a factor $16/12N_f$ from statistics, and a factor $(8/7+2)/2$ from Bose instead of Fermi integrals. Thus

$$\eta_q = \frac{\eta_{qq}}{1+33/7N_f} \simeq 2.2\frac{1+11N_f/48}{1+7N_f/33}N_f\eta_g\,, \tag{31}$$

which for $N_q = 2$ results in $\eta_q = 4.4\eta_g$, a quark viscosity that is larger than the gluon one partly because the gluons generally interact stronger than the quarks and partly because of differences between Bose and Fermi distribution functions.

V. VISCOSITY TO HIGHER ORDERS IN α_S

The leading logarithmic order dominates at extremely high temperatures, where the running coupling constant is small, but at lower temperatures higher orders become important. The next to leading order correction to the viscous rate in the coupling constant is of order α_s^2. It may be significant because the leading logarithm is a slowly increasing function. In the derivation of the leading logarithmic order, Eq. (27), we have been very cavalier with any factors entering in the logarithm, which are of order α_s^2. It was only argued that the leading logarithmic order $\ln(q_{\max}/q_{\min}) \sim \ln(T/q_D)$ because $q_{\max}$ and $q_{\min}$ were of order $\sim T$ and $\sim q_D$, respectively. Finally, if thermal quark-gluon plasmas are created in relativistic heavy-ion collisions at energies reached at CERN and the BNL relativisitic Heavy Ion Collider (RHIC), the temperatures achieved will probably be below a GeV. We can thus estimate the interaction strength from the running coupling constant $\alpha_s \simeq 6\pi/(33-2N_f)\ln(T/\Lambda)$ which, with $\Lambda \simeq 150$ MeV and $T \lesssim 1$ GeV, gives $\alpha_s \gtrsim 0.4$. For such large coupling constants, Debye and dynamical screening is replaced by an effective screening mass $m_{\rm pl}$ as discussed above, which will affect the viscosity considerably.

To calculate the viscosity to order α_s^2 exactly, the 5-dimensional integral of (22) must be evaluated numerically and at the same time a variational calculation of Φ must be performed. This is a very difficult task and we shall instead use the information obtained in the previous section, that the trial function $f \propto p^2$ is expected to be an extremely good approximation. With that ansatz for the trial function, it is then straightforward to calculate the integral of (21) numerically and find the viscosity to order α_s^2 for the given screening mechanism. The 5-dimensional numerical evaluation of the collision integral of (21) is a complicated function of the coupling constant. It is convenient to write it in terms of the function Q:

$$\langle\Phi|I|\Phi\rangle_{gg} = \frac{2^7\pi^3}{15}\alpha_s^2 Q\left(\frac{q_{\max}^{(gg)}}{q_{\min}}\right)T^3\,, \tag{32}$$

where the index gg refers to gluon-gluon scattering, but the analogous definitions apply to gluon-quark and

quark-quark scattering. The function Q and the effective maximum and minimum momentum transfers $q_{\max}$ and $q_{\min}$ are given in Appendix B. In weakly interacting plasmas, where the screening is provided by Debye and dynamical screening, the function Q is basically just a logarithm of the ratio of the maximum and minimum momentum transfer, i.e.,

$$Q\left(\frac{q_{\max}}{q_{\min}}\right) = \ln\left(\frac{q_{\max}}{q_{\min}}\right), \quad \alpha_s \lesssim 0.1. \tag{33}$$

By numerical integration we find that the distribution functions lead to an effective cutoff of $q_{\max}^{(gg)} \sim 3T$. This is because the distribution functions are weighted with several powers of particle momenta and thus contribute the most for $p \simeq 3T$. The effective cutoff is slightly larger for quark-gluon and quark-quark scattering because the Fermi distribution functions emphasize larger momenta than the Bose ones. Debye and dynamical screening leads to $q_{\min} \simeq 1.26 q_D$, as described in Eq. (B6) and so, from (B8),

$$Q\left(\frac{q_{\max}^{(gg)}}{q_{\min}}\right) = \ln\left(\frac{0.44}{\alpha_s(1+N_f/6)}\right), \quad \alpha_s \lesssim 0.1. \tag{34}$$

The numerical factor inside the logarithm, which gives the order α_s^2, is discussed in more detail in Appendix B.

In the other limit, $q_D \gtrsim T$, or equivalently $\alpha_s \gtrsim 0.1$, perturbative ideas break down and we assume an effective screening mass taken from lattice calculations, $q_{\min} \simeq 1.1T$, as described by Eq. (11). Thus we find [see (B10)]

$$Q(q_{\max}^{(gg)}/q_{\min}) = 0.626, \quad \alpha_s \gtrsim 0.1, \tag{35}$$

and similarly for quark-gluon and gluon-gluon scattering $Q(q_{\max}^{(gq)}/q_{\min}) = 0.819$ and $Q(q_{\max}^{(qq)}/q_{\min}) = 1.024$, respectively.

Adding gluon-gluon and gluon-quark scatterings we obtain the gluon viscosities

$$\eta_g = \frac{2^5 15 \xi(5)^2}{\pi^7} \frac{T^3}{\alpha_s^2} \left[Q\left(\frac{q_{\max}^{(gg)}}{q_D}\right) + \frac{11N_f}{48} Q\left(\frac{q_{\max}^{(gq)}}{q_D}\right) \right]^{-1}, \tag{36}$$

which extends Eq. (37) to higher orders. In weakly interacting plasmas (36) reduces to

$$\eta_g \simeq 0.342 \frac{T^3}{\alpha_s^2} \left[\ln\left(\frac{0.44}{\alpha_s(1+N_f/6)}\right) + \frac{11N_f}{48} \ln\left(\frac{0.72}{\alpha_s(1+N_f/6)}\right) \right]^{-1}, \quad \alpha_s \lesssim 0.1, \tag{37}$$

to leading orders in α_s. In strongly interacting plasmas we obtain, by inserting (B10) in (32),

$$\eta_g \simeq 0.55 \frac{T^3}{\alpha_s^2} \left[1 + 1.31 \frac{11N_f}{48} \right]^{-1}, \quad \alpha_s \gtrsim 0.1. \tag{38}$$

In Fig. 3 we show the gluon viscosity with the various assumptions for screening. With a dash-dotted curve the result of Eq. (38) assuming a constant screening mass, $m_{\rm pl} = 1.1T$, is shown. With a dashed curve the numerical result assuming Debye and dynamical screening of Eqs. (8) and (9) is shown. For $\alpha_s \lesssim 0.05$ it is given by Eq. (37) to a good approximation, whereas for $\alpha_s \gtrsim 0.05$ the result of Eq. (B4) is better. The final viscosity shown by a full curve is obtained by combining the two limits, i.e., applying Debye and dynamical screening in weakly interacting plasmas when $q_D \lesssim T$, or equivalently $\alpha_s \lesssim 0.1$, but an effective screening mass $m_{\rm pl} = 1.1T$ as given by Eq. (11) when $\alpha_s \gtrsim 0.1$. This corresponds to choosing the smallest value of the viscosities as seen in Fig. 3, i.e., the two limits of Eqs. (37) and (38).

Similarly, adding quark-quark and quark-gluon scatterings we find the quark viscosity

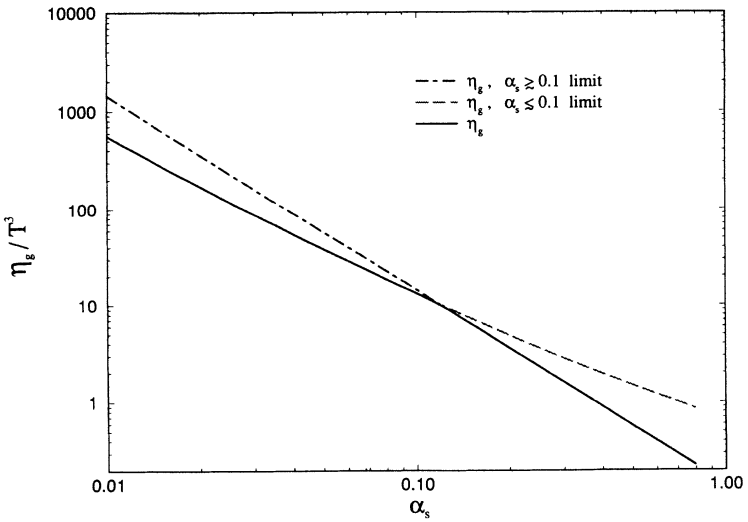

FIG. 3. The gluon viscosity for $N_f = 3$ assuming Debye and dynamical screening (dashed curve), a constant screening mass $m_{\rm pl} = 1.1T$ (dashed-dotted curve), and the minimal one (full curve).

$$\eta_q = \frac{5^3 3^6 \xi(5)^2}{2^3 11 \pi^7} N_f \frac{T^3}{\alpha_s^2} \times \left[Q\left(\frac{q_{\max}^{(qq)}}{q_D}\right) + \frac{7N_f}{33} Q\left(\frac{q_{\max}^{(qq)}}{q_D}\right) \right]^{-1}, \quad (39)$$

which in weakly interacting plasmas gives

$$\eta_q \simeq 0.752 N_f \frac{T^3}{\alpha_s^2} \left[\ln\left(\frac{0.72}{\alpha_s(1+N_f/6)}\right) + \frac{7N_f}{33} \ln\left(\frac{1.15}{\alpha_s(1+N_f/6)}\right) \right]^{-1}, \quad \alpha_s \lesssim 0.1, \quad (40)$$

and, in the strongly interacting plasmas,

$$\eta_q \simeq 0.92 N_f \frac{T^3}{\alpha_s^2} \left[1 + 1.25 \frac{7N_f}{33} \right]^{-1}, \quad \alpha_s \gtrsim 0.1. \quad (41)$$

The quark viscosity increases with the number of quark flavors, N_f, whereas the gluon viscosity decreases as can be seen in Figs. 4 and 5, where the viscosities are shown for two and three flavors, respectively. The total viscosity of a quark-gluon plasma, $\eta = \eta_g + \eta_q$, is dominated by the quark viscosity.

From the definition of the viscosity in terms of the collision integral (18) and (20), which only contains positive quantities, it follows trivially that the viscosity is positive as is a physical necessity. The resulting viscosities of Eqs. (36) and (39) are positive quantities, whereas the $\alpha_s \lesssim 0.1$ expansions of Eqs. (37) and (40) are not when extended to the region $\alpha_s \gtrsim 0.5$. This explains the results found in [14], where it was claimed that estimates of the next to leading order α_s^2 could lead to a negative viscosity.

Contributions from vertex corrections should also be considered. In fact for the calculation of the quasiparticle damping rate γ_p, Braaten and Pisarski [15] found that vertex corrections contributed to leading order $\gamma_{p=0}^{(g)} \simeq 6.6\alpha_s$ for zero gluon momenta, p. Vertex corrections also contribute to order α_s for large quasiparticle momenta, $p \gg gT$, but they can here be ignored since the leading order is $\gamma_p^{(g)} = 3\alpha_s \ln(1/\alpha_s)$ as explained in [16]. For the viscosity vertex corrections can also be ignored since the extra vertices add a factor α_s^2. Even though integration over soft momenta may cancel a factor α_s, as is the case for γ_p, the result is still of higher order in the coupling constant.

Writing each of the viscosities η_i $(i = q, g)$ in terms of the viscous relaxation time $\tau_{\eta i}$ as

$$\eta_i = w_i \tau_{\eta i}/5, \quad (42)$$

where $w_g = (32\pi^2/45)T^4$ and $w_q = (N_f 7\pi^2/15)T^4$ are the gluon and quark enthalpies, respectively, we obtain the viscous relaxation rate for gluons,

$$\frac{1}{\tau_{\eta,g}} = \frac{\pi^9}{3^3 5^3 \xi(5)^2} \frac{T}{\alpha_s^2} \times \left[Q\left(\frac{q_{\max}^{(gg)}}{q_{\min}}\right) + \frac{11N_f}{48} Q\left(\frac{q_{\max}^{(gg)}}{q_{\min}}\right) \right], \quad \alpha_s^2 T, \quad (43)$$

and quarks and antiquarks,

$$\frac{1}{\tau_{\eta,q}} = \frac{11\pi^9 2^3 7}{3^7 5^5 \xi(5)^2} \frac{T}{\alpha_s^2} \times \left[Q\left(\frac{q_{\max}^{(gq)}}{q_{\min}}\right) + \frac{7N_f}{33} Q\left(\frac{q_{\max}^{(qq)}}{q_{\min}}\right) \right], \quad \alpha_s^2 T. \quad (44)$$

The viscous relaxation times, $\tau_{\eta,g}$, $\tau_{\eta,q}$, and $\tau_\eta = 1/(\tau_{\eta,g}^{-1} + \tau_{\eta,q}^{-1})$ are thus very similar to the corresponding viscosities when divided by a factor of T^4. The curves on Figs. 4 and 5 therefore applies to the viscous relaxation times (times temperature) as well when divided by a factor of ~ 1.4 and $\sim 0.92N_f$ for gluons and quarks, respectively, according to Eq. (42).

In weakly interacting plasma the viscous rates can be approximated by

$$\frac{1}{\tau_{\eta,g}} \simeq 4.11 \alpha_s^2 \left[\ln\left(\frac{0.44}{\alpha_s(1+N_f/6)}\right) + \frac{11N_f}{48} \ln\left(\frac{0.72}{\alpha_s(1+N_f/6)}\right) \right], \quad \alpha_s \lesssim 0.1, \quad (45)$$

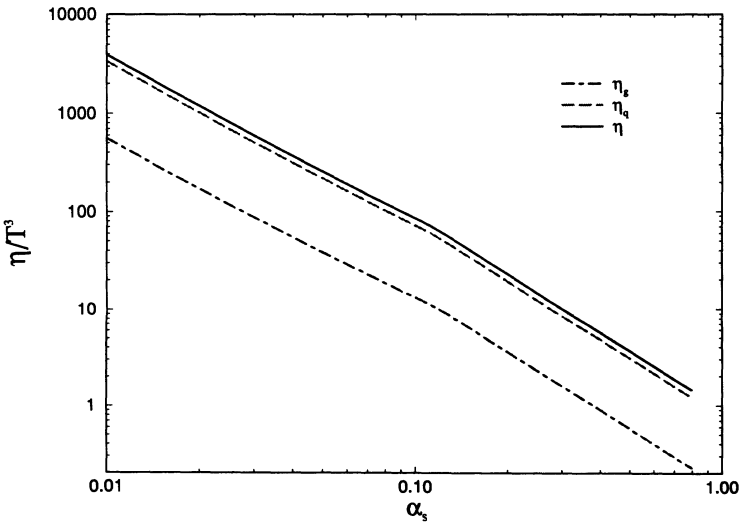

FIG. 4. The quark, gluon, and total viscosities for $N_f = 3$.

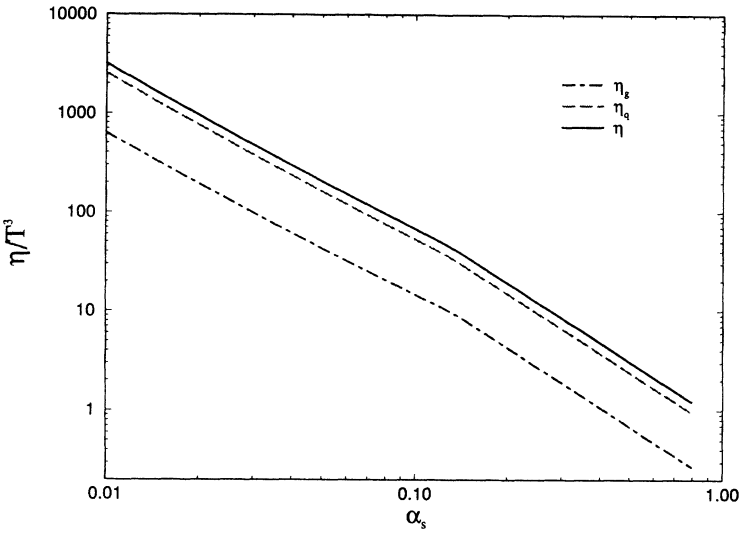

FIG. 5. The quark, gluon, and total viscosities for $N_f = 2$.

and

$$\frac{1}{\tau_{\eta,q}} \simeq 1.27\,\alpha_s^2 \left[\ln\left(\frac{0.72}{\alpha_s(1+N_f/6)}\right) + \frac{7N_f}{33}\ln\left(\frac{1.15}{\alpha_s(1+N_f/6)}\right)\right], \quad \alpha_s \lesssim 0.1\,, \tag{46}$$

to leading orders in α_s.

VI. SUMMARY

By solving the Boltzmann equation for quarks and gluons the viscosities in quark-gluon plasmas were calculated to leading orders in the coupling constant. Inclusion of dynamical screening of transverse interactions, which controls the infrared divergences in QED and QCD, is essential for obtaining finite transport coefficients in the weakly interacting plasmas. The solution of the transport process was extended to strongly interacting plasmas by assuming an effective screening mass of order $m_{\rm pl} = 1.1T$, as found in lattice calculations, when the Debye screening length became larger than the interparticle distance or when $\alpha_s \gtrsim 0.1$. The Boltzmann equation was solved exactly to leading logarithmic order numerically, but the result only differed by less than a percent from an analytical result obtained by a simple ansatz for the deviation from local equilibrium, $\Phi \propto p_x p_y$. The next to leading orders were also calculated and found to be very important for the transport properties relevant for quark-gluon plasmas created in relativistic heavy-ion collisions and the early Universe. For $\alpha_s \gtrsim 0.1$ we find $\eta_i = C_{i,1}T^3/\alpha_s^2 \ln(C_{i,2}/\alpha_s)$, whereas for $\alpha_s \lesssim 0.1$ we find $\eta_i = C_{i,3}T^3/\alpha_s^2$ with coefficients $C_{i,j}$ given above.

The viscosity in degenerate plasmas of quarks, i.e., for $T \ll \mu_q$ was calculated in [6]. Several differences were found. In the high-temperature quark-gluon plasma the chemical potential can be ignored and the transport processes depend on two momentum scales only, namely T and $q_D \sim gT$. In degenerate quark matter three momentum scales enter, namely μ_q, T, and $q_D \sim g\mu_q$, and the transport process depends considerably on which of q_D and T is the larger. In fact for $T \ll q_D$ transverse interactions turn out to be dominant in contrast to the high-temperature quark-gluon plasma where transverse and longitudinal interactions contribute by similar magnitude. Furthermore, the existence of a relative sharp Fermi surface allows an almost analytical calculation of both the leading (logarithmic) order as well as the next order α_s^2.

The techniques for calculating the viscosities to leading orders in the coupling constants can be applied to other transport coefficients as well. The leading logarithmic orders to momentum stopping, electrical conductivities, and thermal dissipation in QCD and QED plasmas have been estimated with simple *Ansätze* for the distribution functions in [5]. Based on the experience with the viscosity studied here, we do not expect the leading logarithmic order for these transport coefficients to decrease by much when a full variational calculation is performed. The next to leading logarithmic order to these transport coefficients can also be estimated in the following way. As for the viscosity, Eq. (B5), one should in the leading logarithm, $\ln(q_{\rm max}/q_{\rm min})$, replace $q_{\rm max}$ by the average particle momenta which enter the collision integral for the relevant transport process, and replace $q_{\rm min}$ by $\sim q_D$.

A few transport coefficients are, however, different. The second viscosity ζ is zero for a gas of massless relativistic particles [1] and one cannot define a thermal conductivity in a plasma of zero baryon number. One can, however, consider thermal dissipation processes [5] where the leading orders also can be calculated with the above methods. The effective soft cutoff will, however, be different for thermal dissipation processes as described in [6] because the transport of energy introduces dependences on ω, which also is present in the transverse screening, $\Pi_T(\omega/q)$.

All the transport processes discussed above depend only on momentum scales from the typical particle momentum, $q_{\rm max} \sim T$ down to the Debye screening wave

number $q_{\min} \sim q_D \sim gT$, which also is the momentum scale for dynamical screening. There is, however, a shorter momentum scale of order of the magnetic mass, $m_{\rm mag} \sim g^2T$, at which perturbative ideas of the quark-gluon plasma fails [17]. As shown in [16] the quark and gluon quasiparticle decay rates depend on this infrared cutoff $m_{\rm mag}$. Furthermore, recent studies [18] find that the color diffusion and conductivity also depend on this cutoff and therefore the rate of color relaxation is a factor $1/\alpha_s$ larger than Eq. (1).

ACKNOWLEDGMENTS

This work was supported by the Director, Office of Energy Research, Office of High Energy and Nuclear Physics, Division of Nuclear Physics, of the U.S. Department of Energy under Contract No. DE-AC03-76SF00098, NSF Grant No. PHY 89-21025, and the Danish Natural Science Research Council. Discussions with Gordon Baym and Chris Pethick are gratefully acknowledged.

APPENDIX A: EXACT VARIATIONAL CALCULATION TO LEADING LOGARITHMIC ORDER

In this appendix we solve the Boltzmann equation and find the deviation from local equilibrium, Φ, by a variational treatment of Eq. (18).

For a general function $\Phi = \hat{\mathbf{p}}_x\hat{\mathbf{p}}_y f(p/T)$ we have

$$\begin{aligned}\Phi_1+\Phi_2-\Phi_3-\Phi_4 &= \hat{\mathbf{p}}_{1,x}\hat{\mathbf{p}}_{1,y}f(p_1)+\hat{\mathbf{p}}_{2,x}\hat{\mathbf{p}}_{2,y}f(p_2)-\hat{\mathbf{p}}_{3,x}\hat{\mathbf{p}}_{3,y}f(p_3)-\hat{\mathbf{p}}_{4,x}\hat{\mathbf{p}}_{4,y}f(p_4)\\ &= -(\hat{\mathbf{q}}_x\hat{\mathbf{p}}_y+\hat{\mathbf{q}}_y\hat{\mathbf{p}}_x)f(p)-\mu\hat{\mathbf{p}}_x\hat{\mathbf{p}}_y f_1(p)+(\hat{\mathbf{q}}_x\hat{\mathbf{p}}'_y+\hat{\mathbf{q}}_y\hat{\mathbf{p}}'_x)f(p')+\mu\hat{\mathbf{p}}'_x\hat{\mathbf{p}}'_y f_1(p')\,, \qquad \text{(A1)}\end{aligned}$$

where we have changed the notation to $\mathbf{p} = \mathbf{p}_1 + \mathbf{q}/2 = \mathbf{p}_3 - \mathbf{q}/2$ and $\mathbf{p}' = \mathbf{p}_2 - \mathbf{q}/2 = \mathbf{p}_4 + \mathbf{q}/2$. We have seen that the energy-conserving δ functions of (21) implies $\hat{\mathbf{p}}\hat{\mathbf{q}} = \hat{\mathbf{p}}'\hat{\mathbf{q}} = \mu$. Furthermore, we have defined the function

$$f_1(p) = p^3 d(f/p^2)/dp = pf' - 2f\,, \qquad \text{(A2)}$$

that vanishes when $f \propto p^2$, which was the case for the ansatz used in Sec. V.

For small momentum transfer the matrix element (3) depends only on energy and momentum transfer and the azimuthal angle ϕ. The δ functions of (21) taking care of energy conservation fixes the polar angles θ_1 and θ_2 with respect to $\mathbf{q}$. Thus all the angular integrals for fixed μ and ϕ reduces to rotating the three vectors $\mathbf{q}$, $\mathbf{p}$, and $\mathbf{p}'$ over all Euler angles keeping them fixed relatively to each other. Only $(\Phi_1+\Phi_2-\Phi_3-\Phi_4)^2$ depends on the Euler angles and the integration or averaging over the three Eulerian angles, while keeping the relative positions of the vectors $\mathbf{q}$, $\mathbf{p}$, and $\mathbf{p}'$ fixed, i.e., keeping μ and ϕ fixed, gives

$$\overline{(\hat{\mathbf{q}}_x\hat{\mathbf{p}}_y+\hat{\mathbf{q}}_y\hat{\mathbf{p}}_x)^2} = \overline{(\hat{\mathbf{q}}_x\hat{\mathbf{p}}'_y+\hat{\mathbf{q}}_y\hat{\mathbf{p}}'_x)^2} = \frac{3+\mu^2}{15}\,, \qquad \text{(A3)}$$

$$\overline{(\hat{\mathbf{p}}_x\hat{\mathbf{p}}_y)^2} = \overline{(\hat{\mathbf{p}}'_x\hat{\mathbf{p}}'_y)^2} = \frac{1}{15}\,, \qquad \text{(A4)}$$

$$\overline{(\hat{\mathbf{q}}_x\hat{\mathbf{p}}_y+\hat{\mathbf{q}}_y\hat{\mathbf{p}}_x)(\hat{\mathbf{p}}_x\hat{\mathbf{p}}_y\mu)} = \frac{2}{15}\mu^2\,, \qquad \text{(A5)}$$

$$\overline{(\hat{\mathbf{q}}_x\hat{\mathbf{p}}'_y+\hat{\mathbf{q}}_y\hat{\mathbf{p}}'_x)(\hat{\mathbf{p}}'_x\hat{\mathbf{p}}'_y\mu)} = \frac{2}{15}\mu^2\,, \qquad \text{(A6)}$$

$$\overline{(\hat{\mathbf{q}}_x\hat{\mathbf{p}}_y+\hat{\mathbf{q}}_y\hat{\mathbf{p}}_x)(\hat{\mathbf{q}}_x\hat{\mathbf{p}}'_y+\hat{\mathbf{q}}_y\hat{\mathbf{p}}'_x)} = \frac{1}{15}(3\hat{\mathbf{p}}\hat{\mathbf{p}}'+\mu^2), \qquad \text{(A7)}$$

$$\begin{aligned}\overline{(\hat{\mathbf{q}}_x\hat{\mathbf{p}}_y+\hat{\mathbf{q}}_y\hat{\mathbf{p}}_x)(\hat{\mathbf{q}}'_y\hat{\mathbf{p}}'_x)} &= \overline{(\hat{\mathbf{q}}'_x\hat{\mathbf{p}}'_y+\hat{\mathbf{q}}'_y\hat{\mathbf{p}}'_x)(\hat{\mathbf{q}}_y\hat{\mathbf{p}}_x)}\\ &= \frac{\mu^2}{15}(3\hat{\mathbf{p}}\hat{\mathbf{p}}'-1)\,, \qquad \text{(A8)}\end{aligned}$$

$$\overline{(\hat{\mathbf{q}}_y\hat{\mathbf{p}}_x)(\hat{\mathbf{p}}'_x\hat{\mathbf{p}}'_y\mu^2)} = \frac{\mu^2}{30}(3(\hat{\mathbf{p}}\hat{\mathbf{p}}')^2-1)\,, \qquad \text{(A9)}$$

where $\hat{\mathbf{p}} = \mathbf{p}/\epsilon_p$ and $\hat{\mathbf{p}}' = \mathbf{p}'/\epsilon'_p$. Since we assume that the plasma temperature is much larger than any of the particle masses, the particles are relativistic and $\hat{\mathbf{p}}$, $\hat{\mathbf{p}}'$, and $\hat{\mathbf{q}}$ are unit vectors. The vector product of $\hat{\mathbf{p}}$ and $\hat{\mathbf{p}}$ is most useful in terms of μ and ϕ (see Fig. 2)

$$\hat{\mathbf{p}}\hat{\mathbf{p}}' = \mu^2 + (1-\mu^2)\cos\phi\,. \qquad \text{(A10)}$$

Next we integrate over μ and ϕ. The μ integration averages μ^2 to $1/3$, whereas the ϕ integration is weighted by a factor $(1-\cos\phi)^2$ from the matrix elements. Thus we find that (A7)–(A9) vanishes whereby all combinations mixing p_1 and p_2 very conveniently disappear. After averaging over both Euler angles and μ and ϕ we obtain

$$\begin{aligned}\langle\overline{(\Phi_1+\Phi_2-\Phi_3-\Phi_4)^2}\rangle &= \frac{q^2}{p^2}\frac{1}{15}(10f^2+f_1^2+4ff_1)\\ &= \frac{q^2}{p^2}\frac{2}{5}(f^2+\frac{1}{6}p^2f'^2)\,. \qquad \text{(A11)}\end{aligned}$$

Let us first consider the pure gluon plasma for which (23) gives

$$\begin{aligned}\langle\Phi|I|\Phi\rangle &= \frac{8\pi}{15}g^4\ln(T/q_D)T^3\\ &\times\int_0^\infty\left[f^2+\frac{1}{6}p^2f'^2\right]\left(-\frac{\partial n}{\partial\epsilon_p}\right)dp\,, \qquad \text{(A12)}\end{aligned}$$

where $n = [\exp(p/T)-1]^{-1}$ is the gluon distribution function. Since

$$\langle\Phi|X\rangle = \frac{8}{15\pi^2}\int fp^3\left(-\frac{\partial n}{\partial\epsilon_p}\right)dp\,, \qquad \text{(A13)}$$

we find, from (18),

$$\eta = \frac{15}{8\pi g^4}\frac{T^3}{\ln(T/q_D)}\frac{\left(\int_0^\infty fn'x^3dx\right)^2}{\int_0^\infty (f^2+\frac{1}{6}x^2f'^2)n'dx}, \quad \text{(A14)}$$

where $x = p/T$. As mentioned above, the function $f(x)$ is determined by minimizing (A14). A functional variation with respect to f results in a second-order inhomogeneous differential equation for f:

$$f'' + \left(\frac{2}{x} + \frac{n''}{n'}\right)f' - \frac{6}{x^2}f = -\tilde{C}x\,, \quad \text{(A15)}$$

where $n''/n' = -(1+2n)$. $\tilde{C}$ is an arbitrary constant that, by rescaling f, can be chosen as $\tilde{C} = 2$ for convenience.

For $x \gg 1$ we can approximate $n \simeq 0$, and so we find the solution to (A15), that does not increase exponentially for $x \to \infty$, to be

$$f(x) = x^2\,, \quad x \gg 1\,. \quad \text{(A16)}$$

For $x \ll 1$ we can approximate $n \simeq 1/x$, and the solution to (A15) that is finite at the origin is

$$f(x) = x^3\left(C - \frac{1}{5}\ln x\right)\,, \quad 0 \le x \ll 1\,, \quad \text{(A17)}$$

where $C \simeq 0.7$ is a constant that can only be determined by finding the full solution to (A15) and matching it to (A17). This is done by a numerical Runge-Kutta integration and the result is shown in Fig. 6. The viscosity is now found by inserting f in (A14). The exact value for η thus obtained is only 0.523% less than the approximate value η_{gg} of Eq. (38). Since the exact value is a variational minimum, it has to be smaller than that of (28). It is only slightly less because $f \simeq x^2$ for large x as the ansatz of (24), and f is mainly sampled over values of $x = p/T \gg 1$ because the integrals over p_1 and p_2 in (23) have powers $\sim p^4$ to $\sim p^5$ times $n_p(1+n_p)$. In Ref. [4] a variational calculation with trial functions $f(p) \propto p^\nu$ lead to a minimal viscosity for $\nu = 2.104$. This result is close to the quadratic power of (A16), but tends slightly towards the asymptotic form of (A17) (see also Fig. 6). It has almost the same slope and curvature as the exact solution around $p = 5T$. (Note that the absolute value is unimportant since it cancels in the viscosity.) The corresponding viscosity was 0.364% smaller than that of (28), i.e., in between the exact result and the ansatz $f \propto x^2$.

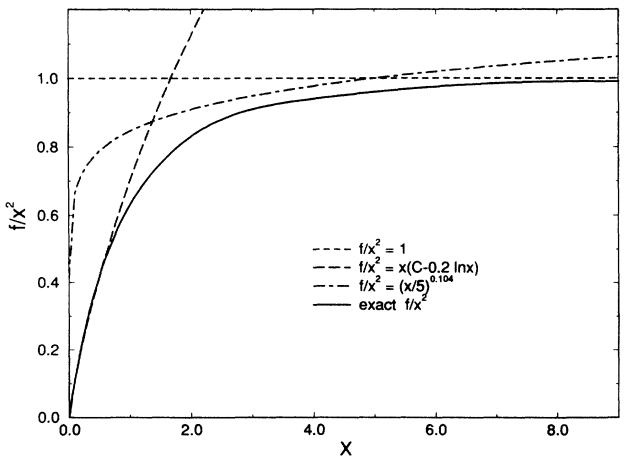

FIG. 6. The function f/x^2 as determined by (A15). Also shown are the limits of (A16), (A17), and the simple *Ansatz* $f = x^2$.

The above analysis was restricted to a pure glue plasma. As mentioned above the distribution functions are weighted with several powers of momentum, and we do not find much difference between fermions and bosons. Therefore the deviation from local equilibrium for quarks will not be much different from gluons, and we can be confident that the ansatz, $\Phi \propto p_x p_y$, of Eq. (24) will be a good approximation for quarks as well as accurate within less than a percent.

APPENDIX B: SOFT AND HARD CONTRIBUTIONS

The essential contribution to $\langle\Phi|I|\Phi\rangle$ is the integral

$$Q\left(\frac{q_{\max}}{q_{\min}}\right) = \frac{1}{3}\int_{-1}^{1}d\mu\int_0^{q_{\max}}q^3\,dq\left[\frac{1}{|q^2+\Pi_L(\mu)|^2} + \frac{1/2}{|q^2+\Pi_T(\mu)/(1-\mu^2)|^2}\right]. \quad \text{(B1)}$$

For dimensional reasons the function Q can only depend on the ratio of $q_{\max}$ to the momentum scale, $q_{\min}$, which is provided by the screening. For Debye and dynamical screening $q_{\min} \sim q_D$, whereas lattice calculations of strongly interacting plasmas give $q_{\min} \sim m_{\rm pl} = 1.1T$.

As described in connection with screening, nonperturbative effects become important when $q_D \gtrsim T$, which corresponds to $\alpha_s \lesssim 0.1$. We shall treat the two limits separately starting with the weakly interacting plasmas for which the gluon self-energies $\Pi_{L,T}(\mu)$ are given by Eqs. (8) and (9). It is straightforward to calculate Q numerically and the result will be given below, but let us first make a simple analytical estimate. The main contribution to this integral can be obtained by including the leading terms in the self-energies (8,9):

$$\Pi_L(q,\omega) \simeq q_D^2\,, \quad \text{(B2)}$$

$$\Pi_T(q,\omega) \simeq i\frac{\pi}{4}\mu q_D^2\,. \quad \text{(B3)}$$

Thus we find for (B1)

$$Q\left(\frac{q_{\max}}{q_{\min}}\right) = \frac{1}{3}\left[\ln\left(1+\frac{q_{\max}^2}{q_D^2}\right) - \frac{q_{\max}^2}{q_D^2+q_{\max}^2} + \frac{1}{4}\ln\left(1+\frac{q_{\max}^4}{q_D^4}\left(\frac{4}{\pi}\right)^2\right) + \frac{2}{\pi}\frac{q_{\max}^2}{q_D^2}\arctan\left(\frac{\pi}{4}\frac{q_D^2}{q_{\max}^2}\right)\right]. \quad \text{(B4)}$$

Expanding in the limit $q_{\max} \gg q_D$ or equivalently for small α_s we obtain the leading orders up to α_s^2 in the coupling constant

$$Q\left(\frac{q_{\max}}{q_{\min}}\right) \simeq \ln\left(\frac{q_{\max}}{q_{\min}}\right)\,, \quad q_{\max} \gg q_D\,, \quad \text{(B5)}$$

where

$$q_{\min} = q_D \exp\left[\frac{1}{6}\left(1 - \ln\frac{4}{\pi}\right)\right] \simeq 1.13 q_D \,. \tag{B6}$$

The two terms in (B5) corresponding to $\ln q_{\max}$ and $\ln q_{\min}$ are often referred to as "hard" and "soft" contributions in the literature [14].

A numerical evaluation of (B1) with $\Pi_{L,T}$ given by Eqs. (8) and (9) instead of (B2) and (B3) gives a slightly larger value for the effective minimum momentum transfer,

$$q_{\min} = 1.26 q_D \,, \tag{B7}$$

because the additional terms in $\Pi_{L,T}$ lead to some additional screening in addition to the Debye screening and Landau damping of (B2) and (B3). This effective cutoff is determined by the screening only and is therefore the same for gluon-gluon, quark-gluon, and quark-quark scattering. Whereas $q_{\min}$ may serve as an effective "cutoff" of small momentum transfer interactions, it is not a parameter put in by hand as discussed in [19]. Contrarily, it is caused and determined by Debye and dynamical screening.

If the transverse interactions are assumed to be Debye screened like the longitudinal ones, i.e., $\Pi_T = q_D^2$, then the result would have been $q_{\min} = q_D \exp(0.5) = 1.65 q_D$. This is because dynamical screening of Eq. (B3) is less effective than the Debye screening of (B2) and thus results in a smaller $q_{\min}$.

It is convenient to express the results in terms of α_s. In weakly interacting plasmas we find

$$Q\left(\frac{q_{\max}}{q_{\min}}\right) \simeq \ln\left(\frac{q_{\max}}{1.26 q_D}\right) = \frac{1}{2}\ln\left(\frac{(q_{\max}/T)^2}{4\pi\alpha_s(1+N_f/6)}\right), \quad \alpha_s \lesssim 0.1. \tag{B8}$$

The upper effective cutoff $q_{\max}$ is provided by the quark and gluon distribution functions as discussed in connection with Eq. (22) and it therefore varies somewhat with particle type. Because Bose distribution functions emphasize smaller momenta than Fermi ones, $q_{\max}$ is larger for quarks. We find $q_{\max}^{(gg)} = 3.0T$, $q_{\max}^{(gq)} = 3.8T$, and $q_{\max}^{(qq)} = 4.8T$ for gluon-gluon, quark-gluon, and quark-quark scattering, respectively. The lower effective cutoff $q_{\min}$ is, however, the same for the three cases because it only depends on the screening in the gluon propagator. Furthermore, we find that the extra terms in the matrix elements of (3), (4), and (5) in addition to the t^{-2} part do not contribute much since they have varying signs and turn out to be partially canceling. Thus the constants within the logarithms of (37) and (40) just reflect the different $q_{\max}$ for gluon-gluon, gluon-quark, and quark-quark scattering.

Lacking screening of transverse interactions in the static limit, it has often been assumed that some mechanism like Debye screening might lead to screening of transverse interactions as well, i.e., $m_{\rm pl} = q_D$. Recently, lattice gauge calculations of QCD plasmas have found effective screening masses of order $m_{\rm pl} \simeq 1.1T$ near the phase transition point, $T_c \simeq 180$ MeV. In both cases it is thus assumed that

$$\Pi_L = \Pi_T/(1-\mu^2) = m_{\rm pl} \tag{B9}$$

in (B1) which leads to

$$Q\left(\frac{q_{\max}}{q_{\min}}\right) = \frac{1}{2}\left[\ln\left(1 + \frac{q_{\max}^2}{m_{\rm pl}^2}\right) - \frac{q_{\max}^2}{m_{\rm pl}^2 + q_{\max}^2}\right]. \tag{B10}$$

With $q_{\max}^{(gg)} = 3.0T$, $q_{\max}^{(gq)} = 3.8T$, $q_{\max}^{(qq)} = 4.8T$, and $m_{\rm pl} = 1.1T$ we find $Q(q_{\max}^{(gg)}/q_{\min}) = 0.626$, $Q(q_{\max}^{(gq)}/q_{\min}) = 0.819$, and $Q(q_{\max}^{(qq)}/q_{\min}) = 1.024$. These values enter the $\alpha_s \gtrsim 0.1$ expressions of Eqs. (38) and (41).

[1] S. Gavin, Nucl. Phys. **B435**, 826 (1984).

[2] A. Hosoya and K. Kajantie, Nucl. Phys. **B250**, 666 (1984).

[3] P. Danielewicz, Phys. Lett. **146B**, 168 (1984).

[4] G. Baym, H. Monien, C. J. Pethick, and D. G. Ravenhall, Phys. Rev. Lett. **64**, 1867 (1990); G. Baym, H. Monien, and C. J. Pethick, in *Proceedings of the International Workshop on Gross Properties of Nuclei and Nuclear Excitations XVI Hirschegg, Austria, 1988*, edited by H. Feldmeier (GSI and Institut für Kernphysik, Darmstadt, 1988), p. 128; and C. J. Pethick, G. Baym, and H. Monien, in *Quark Matter '88*, Proceedings of the Seventh International Conference on Ultrarelativistic Nucleus-Nucleus Collisions, Lenox, Massachusetts, 1988, edited by G. Baym, P. Braun-Munzinger, and S. Nagamiya [Nucl. Phys. **A498**, 313c (1989)].

[5] G. Baym, H. Monien, C. J. Pethick, and D. G. Ravenhall, Nucl. Phys. **A525**, 415c (1991); G. Baym, H. Heiselberg, H. Monien, C. J. Pethick, and J. Popp, in *Quark Matter '91*, Proceedings of the Ninth International Conference on Ultrarelativistic Nucleus-Nucleus Collisions, Gatlinburg, Tennessee, edited by T. C. Awes *et al.* [Nucl. Phys. **A544**, 569c (1992)].

[6] H. Heiselberg and C. J. Pethick, Phys. Rev. D **48**, 2916 (1993); H. Heiselberg, G. Baym, and C. J. Pethick, in *Strange Quark Matter in Physics and Astrophysics*, Proceedings of the International Workshop, Aarhus, Denmark, 1991, edited by J. Madsen and P. Haensel [Nucl. Phys. B (Proc. Suppl.) **24B**, 144 (1991)].

[7] B. L. Combridge, J. Kripfganz, and J. Ranft, Phys. Lett. **70B**, 234 (1977).

[8] H. A. Weldon, Phys. Rev. D **26**, 1394 (1982).

[9] M. B. Kislinger and P. D. Morley, Phys. Rep. **51**, 63 (1979); O. K. Kalashnikov, Fortschr. Phys. **32**, 525 (1984).

[10] O. K. Kalashnikov, Phys. Lett. B **279**, 367 (1992).

[11] M. Gao, Phys. Rev. D **41**, 626 (1990); A. Irback *et al.*, Nucl. Phys. **B363**, 34 (1991).

[12] L. Xiang and E. Shuryak, SUNY Report No. NTG-93-24 (unpublished).
[13] G. Baym and C. J. Pethick, *Landau Fermi-Liquid Theory: Concepts and Applications* (Wiley, New York, 1991).
[14] M. H. Thoma, Phys. Lett. B **269**, 144 (1991); Phys. Rev. D **49**, 451 (1994).
[15] E. Braaten and R. D. Pisarski, Phys. Rev. D **42**, 2156 (1990).
[16] C. P. Burgess and A. L. Marini, Phys. Rev. D **45**, R17 (1992); A. Rebhan, *ibid.* **48**, 482 (1992); H. Heiselberg and C. J. Pethick, *ibid.* **47**, R769 (1993); R. D. Pisarski, *ibid.* **47**, 5589 (1993).
[17] A. D. Linde, Phys. Lett. **96B**, 289 (1980).
[18] A. Selikhov and M. Gyulassy, Phys. Lett. B **316**, 316 (1993); Report No. CU-TP-610/93 and in [19]; H. Heiselberg, in Ref. [19].
[19] U. Heinz, in Preequilibrium Parton Dynamics in Heavy-Ion Collisions, Proceedings of the Workshop, Berkeley, California, 1993, edited by X.-N. Wang (unpublished).

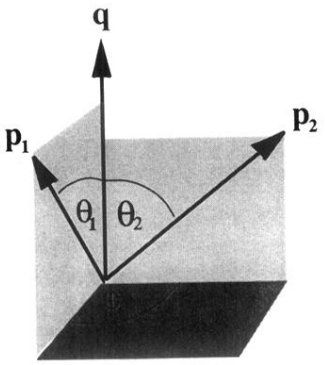

FIG. 2. The collision geometry. For small momentum transfer, $q \ll p_1, p_2$, energy and momentum conservation requires $\cos\theta_1 = \cos\theta_2 = \omega/q$.